ORIGINAL PAPER

Damage Analysis of Sandstone During the Creep Stage After High-Temperature Heat Treatment Based on NMR Technology

Xiaokang Pan[1] · Xiaoping Zhou[1]

Abstract

Based on nuclear magnetic resonance (NMR) technology, the effect of sandstone creep behaviors on porosity is analyzed. Through quantitative analysis of NMR parameters, the distribution of pores of sandstone samples treated at different temperatures during the creep stage is investigated. Moreover, the creep damage mechanism of sandstone is studied by combining the change characteristics of the porosity and the characteristics of creep deformation of sandstone sample during the creep stage. The results show that the creep behavior of sandstone samples promotes an increase in porosity, and the temperature also promotes an increase in the porosity of sandstone during the creep stage. The larger the loading ratio, the more sensitive is the incremental value of porosity to temperature, and the greater is the effect of temperature on creep damage of sandstone samples. When the loading ratio is small, the percentage of micropores decreases and the percentage of macropores increases as the loading ratio increases. However, when the loading ratio is large, the percentage of the micropores increases and the percentage of the macropores decreases as the loading ratio increases. In addition, as the temperature increases, the ductility of sandstone samples increases. Temperature can promote the deformation of sandstone samples during the creep stage, and the effect of temperature on the creep strain is more obvious at high stress levels.

Highlights

- The effects of temperature on the porosity of sandstone during the creep stage are investigated.
- The percentages of the pore distribution of sandstone treated at different temperatures during the creep stage are analyzed.
- The creep damage characteristics of sandstone treated at different temperatures are discussed.
- The relationship between the incremental value of porosity and creep strain is discussed.

1 Introduction

With the development of geothermal energy, oil and gas fields, and coalbed methane, the temperature environment of rocks has changed accordingly. Under these special temperature environments, changes in rock mechanical properties and internal structure directly affect resource extraction. The mechanical properties of rocks often change significantly before and after high-temperature treatment (Inada et al. 1997; Yavuz 2011). Scholars have studied the effect of temperature changes on the mechanical properties of rocks, such as Young's modulus, Poisson's ratio, compressive strength, tensile strength, cohesion and internal friction angle (Dwivedi et al. 2008; Nasseri et al. 2013; Zhao et al. 2012; Liu et al. 2020; Zhou et al. 2020; Gautam et al. 2018; Chen et al. 2012; Ye et al. 2015; Liang et al. 2006). Moreover, some studies have also discussed the effect of thermal changes such as freeze–thaw and thermal shock on the porosity properties of rocks. Akbulut (2022) investigated the changes in physical, mechanical, and microstructural properties of four different colored Ahlat

✉ Xiaoping Zhou
xiao_ping_zhou@126.com

1 School of Civil Engineering, Wuhan University, Wuhan 430072, Hubei, People's Republic of China

ignimbrites under different freeze–thaw cycle conditions. It is concluded that freeze–thaw cycles lead to an increase in the number and size of fractures, cracks and pores, and the deterioration of these microstructures adversely affects the physical and mechanical properties of rocks. Yuan et al. (2022) studied the three-point bending fracture characteristics and dynamic failure characteristics of yellow sandstone treated at 25–800 °C. They found that the P-wave velocity and fracture toughness decreases slightly before the heating temperature reaches 400 °C and then decreases rapidly after 400 °C, while the crack length and peak propagation rate significantly increase with increasing temperature. Guler et al. (2021) studied the physical, mechanical, and index properties of six different carbonate rocks after thermal shock and freeze–thaw effects. They found that as the number of thermal shock and freeze–thaw cycles increases, the degradation of the internal microstructures of the carbonate rocks increases, resulting in a significant decrease in resistance to physical and mechanical actions. Sandstone is a sedimentary rock, mainly composed of various sand grains and is commonly found in a variety of geological mines. Many studies have shown that the mechanical properties of sandstone change after high-temperature treatment. For example, Deng et al. (2021) analyzed the variation law of uniaxial compression strength and peak strain of sandstone after high-temperature treatment. They found that the

uniaxial compressive strength of sandstone increases rapidly with the increase of temperature at 25–500 °C, while the uniaxial compressive strength decreases rapidly at 500–600 °C due to a transition from α-quartz to β-quartz. Zhang et al. (2022) analyzed the pore characteristic change, yield strength, and deformation of the sandstones after high-temperature treatment. They found that when the heating temperature exceeds the threshold of 400 °C, the porosity of sandstone increases rapidly, the yield strength decreases rapidly, and the maximum displacement during the compaction stage increases significantly. Zhang et al. (2021b) studied the effect of temperature on the pore and microstructure of sandstone. They found that when the temperature is 500–1000 °C, the micropores of red sandstone decrease, mesopores and macropores gradually develop, and the compressive strength decreases. However, when the temperature exceeds 1000 °C, the sandstone grains gradually melt and the pores are filled, thereby reducing the porosity. In addition, many studies related to this topic have also been conducted (Zhang et al. 2021a; Li and Liu 2022; Xiao et al. 2021, 2022; Huang et al. 2021; Pathiranagei and Gratchev 2021; Li et al. 2020; Lei et al. 2019). The mechanical properties of sandstone treated at different temperatures are summarized in Table 1.

Analyzing the variation law of creep mechanical behavior of rocks with temperature has important engineering

Table 1 Some data from studies about the mechanical properties of sandstone treated at different temperatures

Rock	Sample size	Temperature range (°C)	Parameters	References
Yellow sandstone from Shandong Province	φ25 mm×50 mm	25, 800, 1000, 1100, 1250	Glossiness, hardness, colour brightness, surface micrographs	Zhang et al. (2021a)
Tight sandstone from Jiulongpo District of Chongqing	φ50 mm×100 mm	25, 200, 400, 600, 800	Mass, volume, porosity, bulk density, mineral composition, Poisson's ratio	Li and Liu (2022)
Sandstone from Weiyuan County of Sichuan Province	50 mm×50 mm×100 mm	200, 350, 500, 650, 800, 950	Density, P-wave velocity, peak strength, peak strain	Xiao et al. (2021)
Red sandstones from Ganzhou, Jiangxi Province	φ50 mm×25 mm	25–1000	Surface features, mass, P-wave velocity, porosity, thermal conductivity, tensile strength	Huang et al. (2021)
Fine-grained sandstone from Jimboomba area, Gold Coast, Australia	φ50 mm×100 mm	25, 200, 400, 600, 800	Porosity, density, compressive strength, elastic modulus, failure modes	Pathiranagei and Gratchev (2021)
Sandstone in Jiangbei District of Chongqing	φ50 mm×100 mm	25, 200, 400, 600, 800, 1000	Brittleness index, peak strength, AE response characteristics, failure patterns	Xiao et al. (2022)
Sandstone from Laohutai Coal Mine in Fushun City, Liaoning Province	φ50 mm×100 mm	25–900	Porosity, permeability, peak strength, peak strain	Li et al. (2020)
Sandstone from Jiulongpo District of Chongqing	φ50 mm×100 mm	25, 200, 400, 600, 800, 900	Peak strength, peak strain, Young's modulus, Poisson's ratio, shear modulus, bulk modulus, pore structure, AE response characteristics	Lei et al. (2019)

significance for revealing the failure mechanism of long-term deformation of rocks under extreme conditions. Scholars have carried out a lot of research on the effect of temperature on creep properties of sandstone. For example, combined with scanning electron microscope, Wang et al. (2019) carried out triaxial rheological test of sandstone. They found that higher temperatures lead to more severe structural failure, which in turn reduces the integrity of the sandstone and improves the rheological response. Yang and Hu (2018) carried out multi-step loading and unloading cycles creep experiments of red sandstone after high-temperature treatment. They analyzed the variation law of strain with temperature, including instantaneous elastic strain, instantaneous plastic strain, viscoelastic strain, viscoplastic strain, and total strain. Pan et al. (2022a, b) studied the effect of temperature on the creep damage behavior of red sandstone based on acoustic emission technology. They found that the proportion of low-energy acoustic emission signal of red sandstone increases exponentially with increasing temperature. In addition, scholars have also made some progress in the study of the creep constitutive models of sandstone treated at high temperature. For example, Li and Yin (2021) proposed a nonlinear viscous pot element and a nonlinear spring element, and replaced linear viscous pot elements and linear spring element in the Nishihara model to obtain an unsteady parameter creep model. They found that the creep model is in good agreement with the actual creep curve of sandstone. Wang et al. (2018) introduces a nonlinear viscous dashpot and proposed a modified Nishihara rheological model based on thermal damage theory. The proposed that the rheological model is suitable for describing the creep curves of sandstone treated at high temperature.

Nowadays, NMR technology has been popularized in life science, food processing, oil extraction, chemistry, agriculture, and other fields. Since the NMR technology is only sensitive to the pore fluid in the porous medium, the pore structure of the porous medium can be obtained by using NMR relaxation. In addition, NMR technology is harmless to the human body, and it has the advantages of high sensitivity, fast detection, non-destructive and so on (Zhou et al. 2021; Cheng et al. 2021; Dillinger and Esteban 2014; Fang et al. 2016; Alam et al. 2014; Yao and Liu 2012; Rios et al. 2011; Li et al. 2015). Therefore, NMR technology is suitable for analyzing the distribution of pores in rocks. However, as a new non-destructive testing method, NMR technology is relatively less used to study the distribution characteristics of pores during rock creep under high-temperature conditions. Therefore, based on NMR technology, the effects of temperature on pore changes of sandstone during the creep stage are investigated in this paper. Combined with pore changes and creep deformation, the micro-damage characteristics of

sandstone treated at different temperatures during the creep stage are analyzed.

2 Material and Methods

2.1 Sample Preparation

The sandstone samples are taken from the same piece of the rock. To ensure that the internal microstructures of the sandstone samples are as close as possible, the samples are processed into a cylinder and those with similar density and appearance are selected. The grain sizes of the sandstone sample are within the range of 0.1–0.5 mm. The main mineral components of sandstone samples include montmorillonite, feldspar, quartz and mica. The average density of the original sandstone samples is 2441 kg/m^3, and the P-wave velocity is 3.53 km/s. The original sandstone samples are first heated in a muffle furnace to a preset temperature (25 °C, 200 °C, 400 °C and 600 °C) at a rate of 10 °C/min and stabilized for 3 h and then cooled at room temperature. Figure 1 shows sandstone samples treated at different temperatures. It can be seen from Fig. 1 that temperature has a significant effect on sandstone samples. As the temperature increases, the color of the sandstone samples gradually darkens. Especially when the temperature is 600 °C, the color of the samples becomes reddish brown. The basic physical parameters of the samples treated at different temperatures are shown in Table 2.

2.2 Experimental Program

The experimental loading device is a triaxial servo-controlled testing machine of Chongqing University (Pan et al. 2020), as shown in Fig. 2. The experimental device consists of a loading system, a triaxial stress chamber, and a data acquisition system. The operation process of the compression experiment is as follows: (a) the sample is first placed in the triaxial stress chamber, which is subsequently sealed; (b) the loading system is operated to achieve an axial stress of 0.5 MPa, so that the sample is pretightened; (c) the sample is loaded at a certain loading speed until it fails; and (d) the data measured by the sensor is transmitted to the computer and finally a digital change is displayed on the computer screen.

Before the experiments, all sandstone samples are saturated with water. The uniaxial compression test is first carried out, and the uniaxial compressive strength (UCS) is obtained when the sample fails. The UCS is used to determine the loading stress for each level in the creep
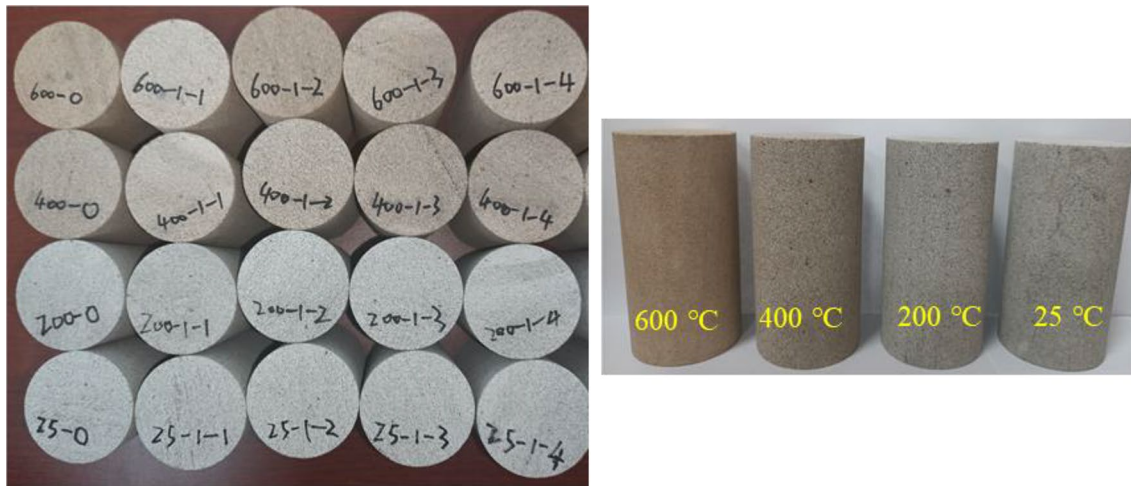
Fig. 1 Sandstone samples treated at different temperatures

Table 2 Summary of basic test results on sandstone samples treated at different temperatures

Rock samples	Diameter (mm)	Height (mm)	Weight (g)	UCS (MPa)
25 °C	48.97	100.46	461.16	30.99
200 °C	48.97	100.38	460.05	36.26
400 °C	49.02	100.56	456.38	38.28
600 °C	49.23	100.45	455.80	47.78

Fig. 2 The experimental loading device

experiments. The test uses displacement loading, and the loading rate is 0.1 mm per second.

The experiment is divided into two parts: compression experiment and creep experiment. For the compression experiment, the sandstone sample is first loaded to each preset stress at a rate of 0.01 kN/s and then unloaded until the stress is zero. The preset stresses of the experiment are 0.5 σ_{ucs}, 0.6 σ_{ucs}, 0.7 σ_{ucs}, and 0.8 σ_{ucs}. The specific loading method in the compression experiment is shown in Fig. 3a. For the creep experiment, the sandstone sample is first loaded to the preset stress at a rate of 0.01 kN/s, and then the stress keeps constant. When the creep time reaches about 8 h, the stress is unloaded to zero. The specific loading method for the creep experiment is shown in Fig. 3b. In the experiment, each sample is first subjected to a compression experiment and then the same sample is subjected to a creep experiment again. The different samples are used for experiments with different preset stress levels. Moreover, uniaxial compression and creep experiments are both carried out at the room temperature, about 25 °C.

A loading ratio is introduced to represent the loading stress level. The loading ratio is the ratio of the preset stress to the uniaxial compressive strength. The expression of load ratio is written as:

$$k = \frac{\sigma_a}{\sigma_{ucs}}, \tag{1}$$

where σ_a is the preset stress, and σ_{ucs} is the uniaxial compressive strength.

The loading ratios and corresponding loading stresses of sandstone samples treated at different temperatures are shown in Table 3.
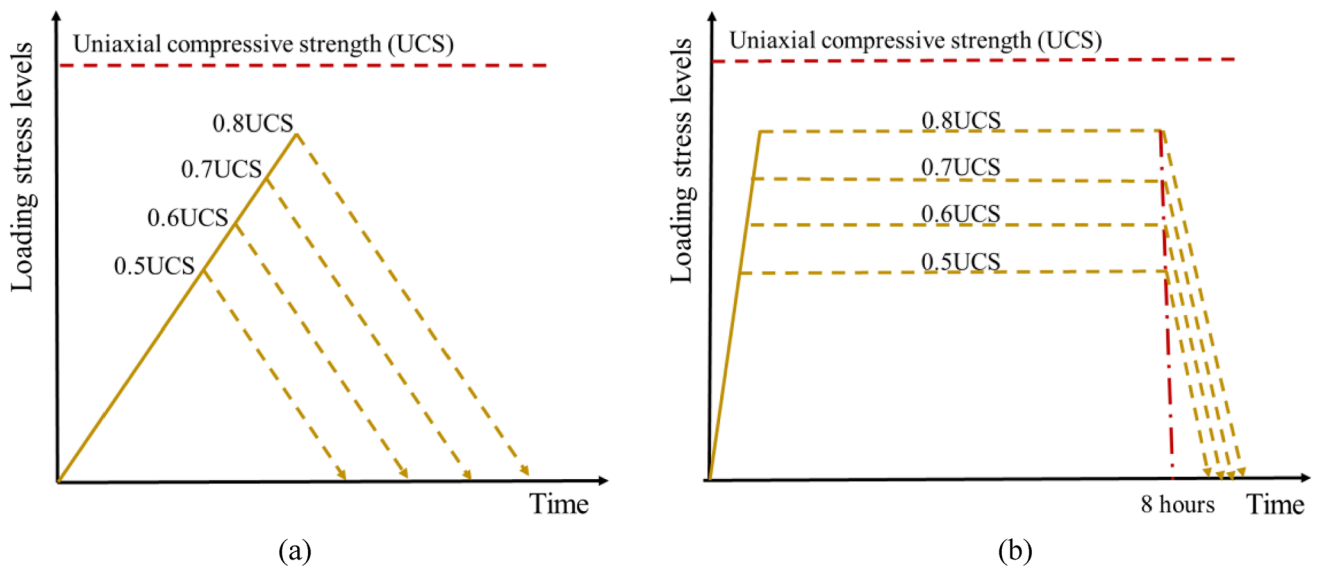
Fig. 3 Loading methods in the experiment. **a** Loading method for the compression experiment. **b** Loading method for the creep experiment

Table 3 The loading ratios (k) and the corresponding loading stresses (σ_a)

k	σ_a (MPa)			
	25 °C	200 °C	400 °C	600 °C
0.5	15.50	18.13	19.14	23.89
0.6	18.59	21.76	22.97	28.67
0.7	21.69	25.38	26.80	33.45
0.8	24.79	29.01	30.62	38.22

2.3 Sample Saturation and NMR Measurements

Before the NMR measurement, the samples must be saturated with water. First, the sandstone samples are placed in a vacuum container with -0.1 MPa and degassed for more than 24 h. Then water is injected into the container so that the samples are saturated with water for more than 12 h in an environment with a water pressure of 1 MPa. The detailed experimental flowchart is shown in Fig. 4.

In addition to NMR measurement, the porosity of samples can be also obtained by the conventional water imbibition (WI) method. Through the mass and volume of the dried sample and saturated sample, the porosity of the sandstone samples can be calculated. The WI porosity is expressed by
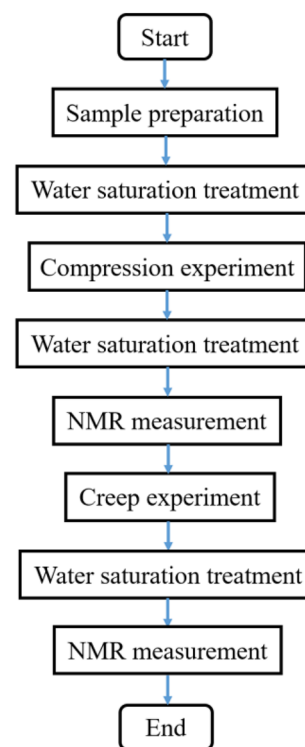

Fig. 4 Flowchart of the experimental procedure

$$\lambda_w = \frac{m_s - m_d}{\rho_w V_r} \times 100\%, \qquad (2)$$

where λ_w is the WI porosity, ρ_w is the density of water, V_r is the volume of sandstone sample, m_s is the mass of the saturated sample, and m_d is the mass of the dried sample.

3 Analysis of the Results

3.1 Validation of the NMR Tests

The paper verifies the accuracy of NMR detection by comparing the WI method with the NMR method. Table 4 shows the porosity obtained by the NMR method and the WI method. The porosity obtained by the WI method is slightly larger than that obtained by the NMR method. This difference is due to the limitations of NMR technology. The NMR technology cannot detect pores smaller than 3 nm due to the extremely fast relaxation of hydrogen in small pores (Daigle et al. 2017). However, it can be seen from the test results that the error between NMR porosity and WI porosity is very small (not more than 1%), so the NMR test result is accurate.

To compare the NMR porosity and WI porosity more intuitively, the NMR porosity and WI porosity are plotted graphically in Fig. 5. The horizontal axis is the WI porosity, and the vertical axis is the NMR porosity. It can be found from Fig. 5 that these points drawn by the NMR porosity and WI porosity are almost located near the angular bisector ($y = x$). It is confirmed that the results obtained by the NMR test are in good agreement with those obtained by the WI method. Therefore, the NMR technology is suitable for detecting the porosity of rocks.
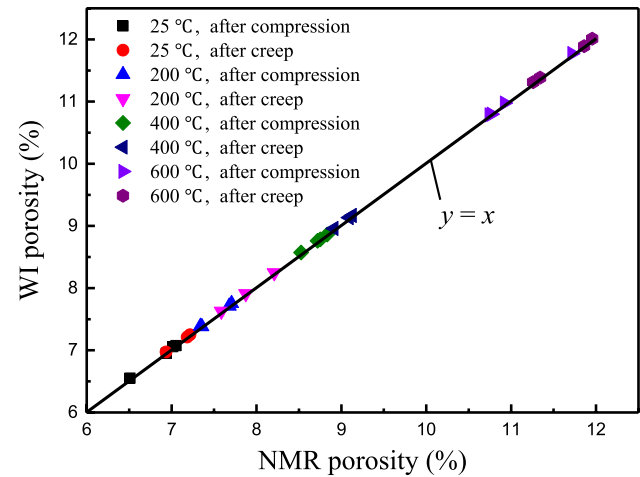

Fig. 5 Comparison of the NMR porosity and WI porosity

3.2 T_2 Spectra Distribution

The NMR technology of rocks is mainly realized by monitoring the relaxation characteristics of hydrogen atoms contained in the pores of saturated samples. The relaxation rate of NMR is very sensitive to the effects of the hydrogen atoms of the fluid in the porous medium, and can reflect the interaction between the fluid and the porous medium. The porosity of different rocks is different, and the position and number of hydrogen atoms reflected by the NMR signal are different. Therefore, according to the NMR signal of hydrogen atoms, it is possible to track the initiate and propagate of cracks in rock samples under different stress conditions. For the fluid

Table 4 Comparison of NMR porosity and WI porosity

Rock type	Loading ratio (k)	After compression		Error (%)	After creep		Error (%)
		NMR porosity (%)	WI porosity (%)		NMR porosity (%)	WI porosity (%)	
25 °C	0.5	7.0525	7.0757	0.3290	7.1837	7.2129	0.4065
	0.6	7.0136	7.0578	0.6302	7.2168	7.2507	0.4698
	0.7	6.5107	6.5526	0.6436	6.9349	6.9717	0.5306
	0.8	6.9375	6.9538	0.2350	–	–	–
200 °C	0.5	7.7064	7.7517	0.5878	7.8744	7.9109	0.4635
	0.6	7.3399	7.3865	0.6349	7.5869	7.6284	0.5470
	0.7	7.6784	7.7107	0.4207	8.2098	8.2473	0.4568
	0.8	7.3565	7.3788	0.3031	–	–	–
400 °C	0.5	8.7191	8.7609	0.4794	8.9119	8.9588	0.5263
	0.6	8.8335	8.8626	0.3294	9.1281	9.1675	0.4316
	0.7	8.5259	8.5729	0.5512	9.0920	9.1339	0.4608
	0.8	8.7521	8.7843	0.3679	–	–	–
600 °C	0.5	11.7162	11.7721	0.4771	11.9555	12.0114	0.4676
	0.6	10.9214	10.9756	0.4963	11.2589	11.3131	0.4814
	0.7	10.7403	10.7852	0.4181	11.3409	11.3858	0.3959
	0.8	10.7661	10.7976	0.2926	11.8593	11.8908	0.2656

in the pores, there are three different relaxation mechanisms, including free relaxation, surface relaxation and diffusion relaxation. In rock pores, the T_2 relaxation time of a fluid can be expressed as

$$\frac{1}{T_2} = \frac{1}{T_{2b}} + \frac{1}{T_{2s}} + \frac{1}{T_{2d}}, \tag{3}$$

where T_{2b} is the lateral relaxation time of the free state fluid, T_{2s} is the lateral relaxation time of the fluid due to surface relaxation, and T_{2d} is the lateral relaxation time of the fluid due to diffusion relaxation under a gradient magnetic field.

In saturated samples, surface relaxation plays a key role, that is, T_2 is directly proportional to the pore size, which can be written as:

$$\frac{1}{T_2} \approx \frac{1}{T_{2s}} = \rho_2 \left(\frac{S}{V}\right)_k, \tag{4}$$

where ρ_2 is the surface relaxation rate of T_2, and $\left(\frac{S}{V}\right)_k$ is the specific surface area of the pores.

The T_2 spectrum can reflect the information about the characteristics of pores. The longer the relaxation time of the water in the pores, the larger is the pore size; the shorter the relaxation time of the water in the pores, the smaller is the pore size. In other words, the relaxation time in the T_2 spectrum is positively correlated with the pore size. The volume of pores and cracks is related to the amplitude of T_2 spectrum. The larger the amplitude, the larger is the total volume of the corresponding pores and cracks.

When the temperatures are 25 °C, 200 °C, 400 °C and 600 °C, the NMR T_2 distributions of the sandstone samples under the different loading ratios are shown in Figs. 6, 7, 8, and 9, respectively. When the temperatures are 25 °C and 200 °C, the T_2 distribution curves of the sandstone samples have two spectral peaks. The pores corresponding to the two spectral peaks are called mesopores and macropores from left to right. When the temperatures are 400 °C and 600 °C, the T_2 distribution curves of the sandstone samples have three spectral peaks. The pores corresponding to the three spectral peaks are called micropores, mesopores, and
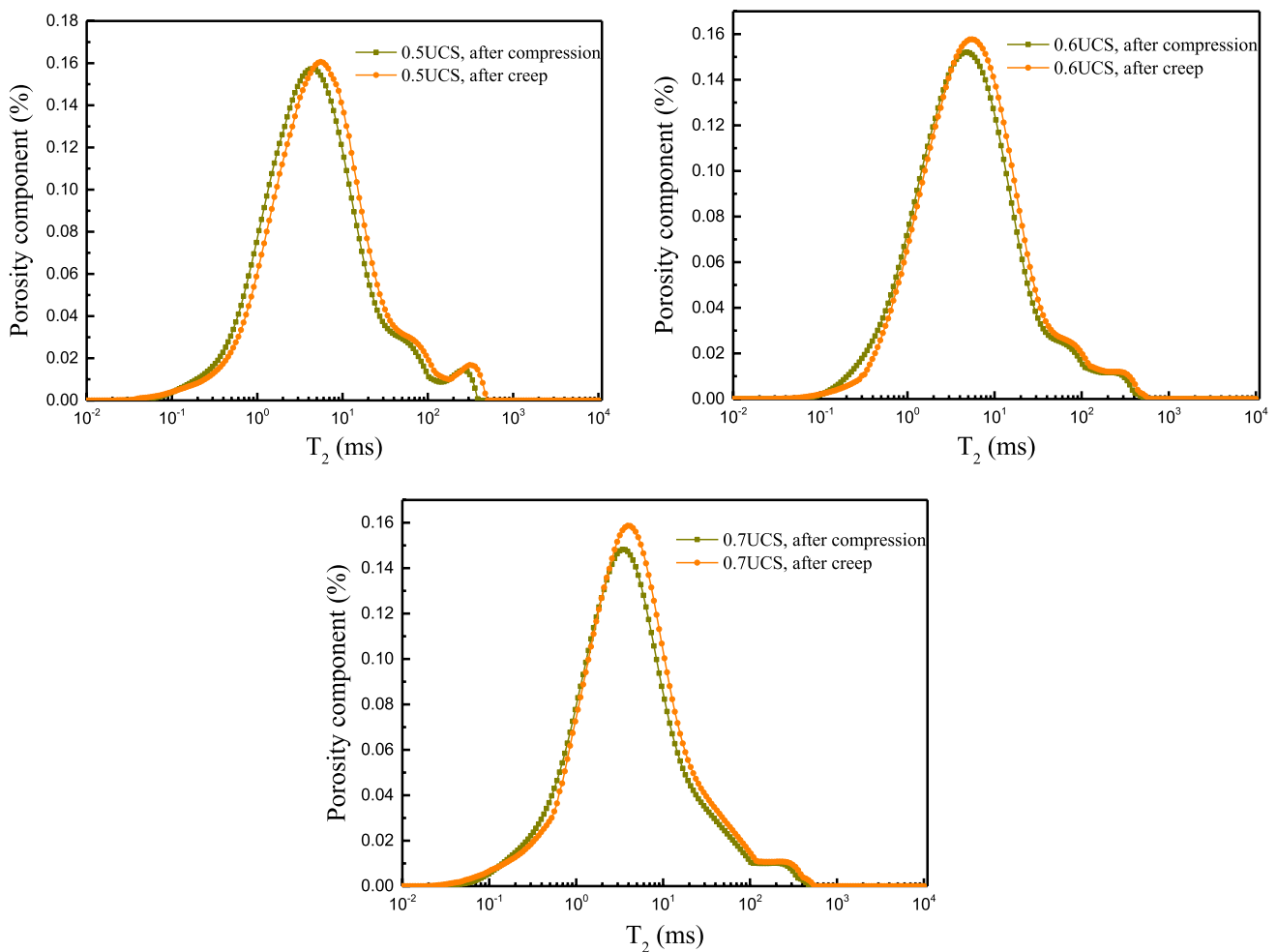

Fig. 6 T_2 distribution of sandstone samples treated at 25 °C
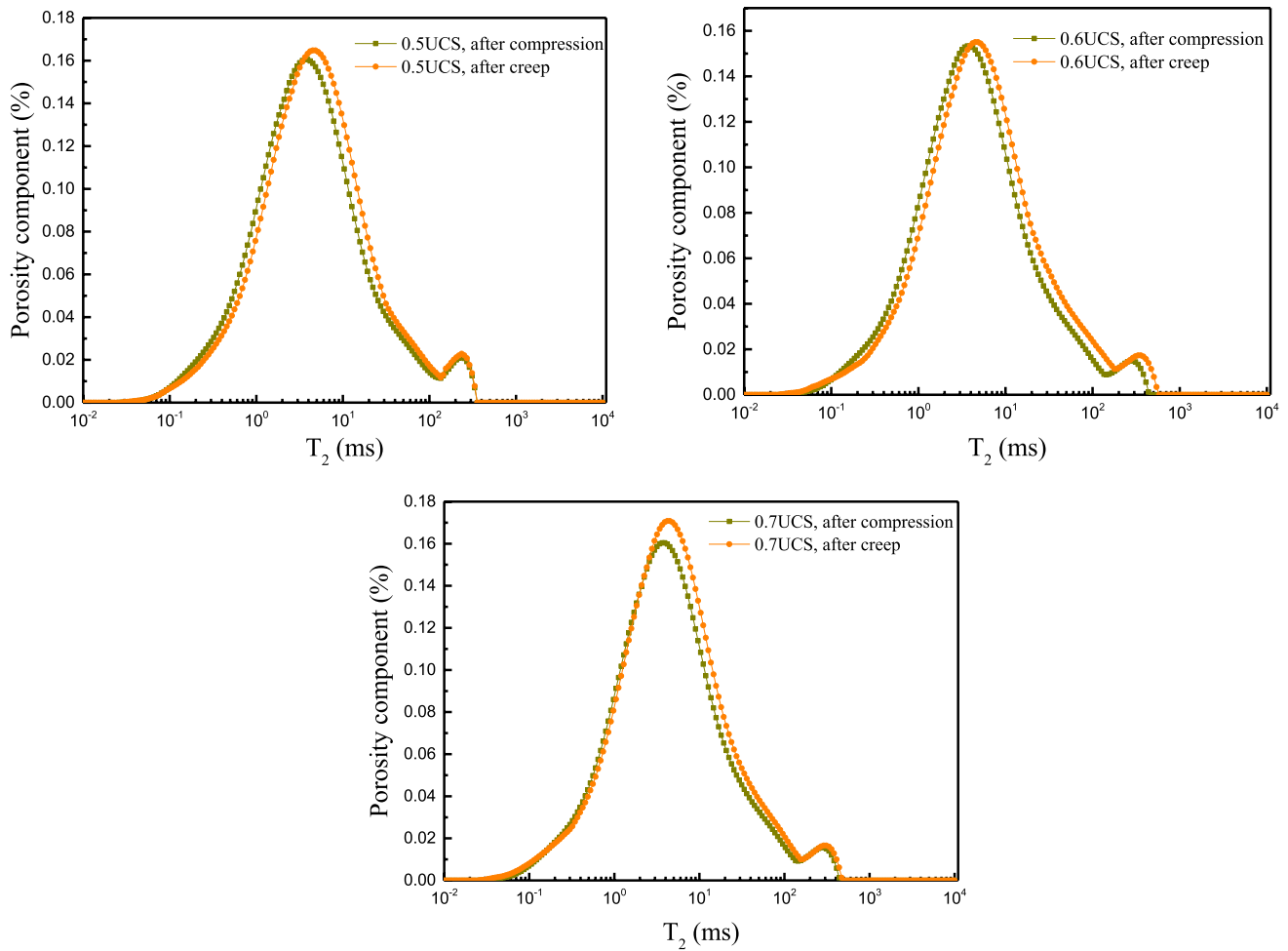
Fig. 7 T_2 distribution of sandstone samples treated at 200 °C

macropores from left to right. As the temperature increases, the spectral peak corresponding to the micropores becomes more obvious. That is, as the temperature increases, the micropores inside the rock increase. In addition, the T_2 distribution curves after creep are all on the right of the T_2 curve after compression. Compared with the spectral peak of the sandstone sample after compression, the spectral peak after creep is larger. This means that the creep behavior of the sandstone sample promotes an increase in porosity. In the process of rock creep, due to the propagation of pores, micropores gradually evolve into mesopores and macropores, leading to a decrease in micropores and an increase in mesopores and macropores.

3.3 Changes in the Porosity of Sandstone Samples

Porosity is one of the important indexes for studying the physical and mechanical properties of rocks (Lia et al. 2018). Porosity refers to the ratio of the sum of all pore volumes in a rock sample to the volume of the rock sample, expressed as a percentage. According to the test result of T_2 spectrum, the porosity of sandstone sample can be obtained. During the creep stage, the change in porosity of sandstone sample is represented by the incremental value of porosity. The incremental value of porosity refers to the difference between the porosity of the sample before creep and the porosity of the sample after creep. Figure 10 shows the incremental value of porosity of sandstone sample treated at different temperatures during the creep stage. Under the same temperature treatment, as the loading ratio increases, the incremental value of porosity of sandstone sample gradually increases. By fitting the incremental value of porosity of the sandstone sample, it can be found that there is a good exponential function relationship between the incremental value of porosity and the loading ratio. The exponential function expression is $P = ae^{bk} + c$, where a, b, and c are the fitting parameters. In addition, it can be seen from Fig. 10 that the higher the temperature, the higher is the exponential function curve. This implies that under the same loading ratio, the greater the temperature, the greater is the incremental value of porosity.
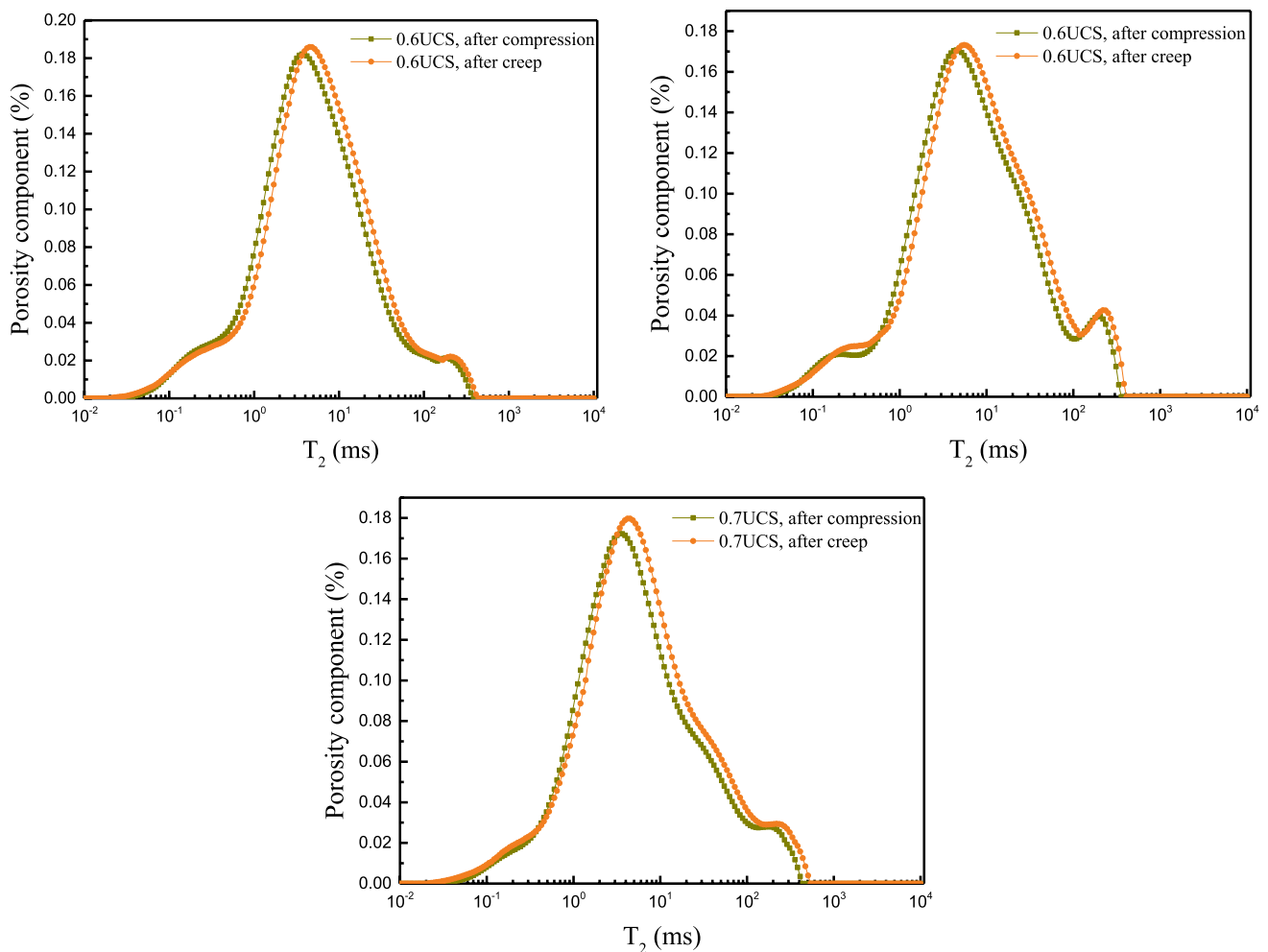
Fig. 8 T_2 distribution of sandstone samples treated at 400 °C

As the loading ratio increases, the incremental value of porosity of the sandstone sample gradually increases, and the incremental rate gradually increases. Especially when the loading ratio exceeds 0.6, the incremental value of porosity increases faster. When the loading ratio is 0.7, as the temperature increases from 25 to 400 °C, the incremental value of porosity is 0.424%, 0.531% and 0.566%, respectively. When the loading ratio is 0.8 and the temperature is 600 °C, the incremental value of porosity reaches 1.093%. It indicates that when the loading ratio exceeds 0.6, severe damage to the sandstone sample is initiated and propagated during the creep stage, and there exists unstable growth of microcracks in the sandstone sample.

Under the same loading ratio, as temperature increases, the incremental value of porosity gradually increases. By fitting the change curve of the incremental value of porosity with temperature, a linear relationship between the incremental value of porosity and the temperature can be obtained, as shown in Fig. 11. It indicates that the temperature promotes the increase of the porosity of sandstone in the creep stage. Moreover, it is found that as loading ratio increases, the incremental rate of porosity increases. When the loading ratios are 0.5, 0.6 and 0.7, the slopes of the corresponding curves are 1.81, 2.34 and 2.90, respectively. It indicates that the larger the loading ratio, the more sensitive is the incremental value of porosity to temperature.

3.4 Damage Characteristics of Sandstone During the Creep Stage

When the rock is affected by external forces, temperature, water, and other factors, cracks or defects occur in the rock, indicating the occurrence of damage. Many ways can be used to define rock damage. Some methods are based on the plastic deformation of the materials or acoustic emission signals to define the damage, and other methods are based on the elastic
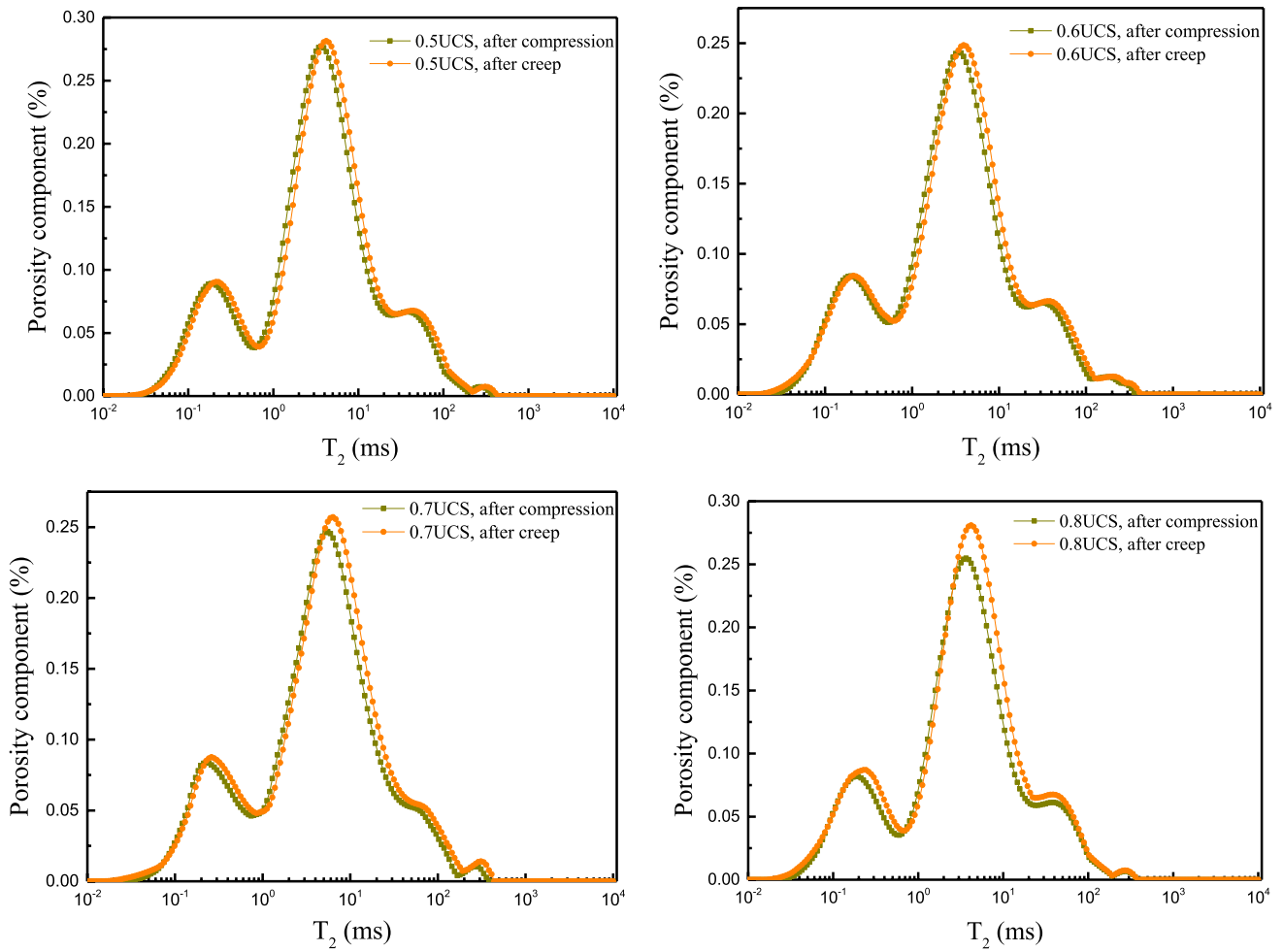
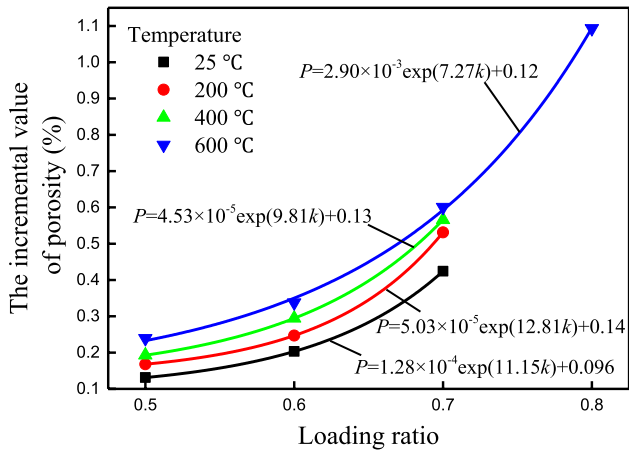**Fig. 9** T_2 distribution of sandstone samples treated at 600 °C

Fig. 10 The incremental value of porosity in the creep stage of the sandstone sample treated with different temperatures
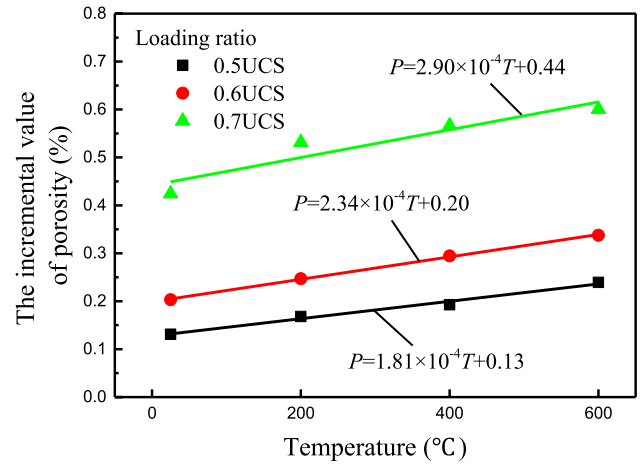

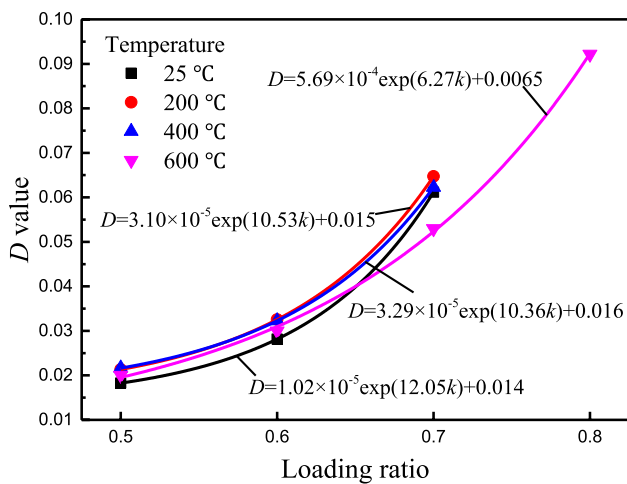**Fig. 11** The relationship between the incremental value of porosity and temperature

Fig. 12 The relationship between D value and loading ratio under different temperatures
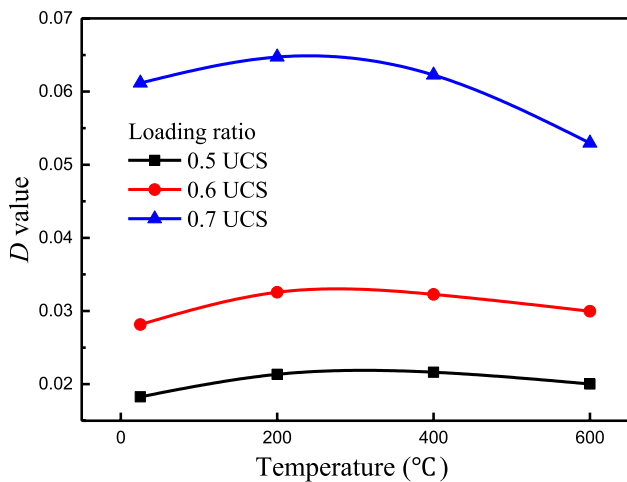

Fig. 13 The relationship between D value and temperature under different loading ratios

modulus of the material to define the damage. This paper defines the damage of sandstone sample in the creep process based on the change of rock porosity. The D value is introduced to quantitatively analyze the damage of the sandstone sample. The D value is written as (Zhou et al. 2021)

$$D = \frac{\Delta P_a^i}{P_a^i} = \frac{P_a^i - P_a^{i-1}}{P_a^i} \quad (i = 1, 2, 3, \ldots), \quad (5)$$

where P_a^i is the porosity of the sandstone sample after the ith creep stage, P_a^0 is the initial porosity of the sandstone sample, and ΔP_a^i is the incremental value of porosity during the ith creep stage.

The D value can well represent the damage caused by the creep behavior to the sandstone sample. Under different loading ratios and temperature conditions, the corresponding D values are different. Figure 12 shows the variation law of D value with loading ratio. It can be found from Fig. 12 that the D value increases exponentially with an increase in the loading ratio, and the greater the loading ratio, the greater is the incremental rate of the D value. Figure 13 shows the variation law of D value with temperature. As the temperature increases, the D value first increases and then decreases. When the temperature increases from 25 to 200 °C, the D value increases. When the temperature increases from 200 to 600 °C, the D value gradually decreases. Moreover, when the loading ratio is 0.7, as the temperature increases from 200 to 600 °C, the D value decreases faster. Such phenomenon indicates that the larger the loading ratio, the greater is the effect of temperature on creep damage of the sandstone sample.

3.5 Percentage of Pore Distribution

The porosity of rocks is an important indicator to describe the rock structure. The test method of porosity of rocks based on NMR technology can accurately determine the proportion of pores with different pore sizes. According to the classification of pore size by NMR theory, the pores in the range of $T_2 < 10$ ms are defined as micropores, and the pores in the range of $T_2 > 10$ ms are defined as macropores (Tang et al. 2016). Based on the division of the pore distribution in the T_2 spectrum, Fig. 14 shows the percentage of the pore of sandstone samples treated at different temperatures after compression and creep experiments. Irrespective of whether after the compression experiment or the creep experiment, the percentage of micropores is relatively large, about 60–80%, while the percentage of macropores is small, about 20–40%.

To analyze the relationship between pore distribution and loading ratio more clearly, Fig. 15 shows the variation law of micropores and macropores with loading ratio. When the temperatures are 25 °C, 200 °C and 400 °C, as the loading ratio increases from 0.5 to 0.6, the percentage of micropores decreases, while the percentage of macropores increases. When the temperature is 600 °C, as the loading ratio increases from 0.5 to 0.7, the percentage of micropores decreases, while the percentage of macropores increases. This phenomenon implies that when the stress level is small, only a small number of newly created micropores are initiated inside the rock, and more number of micropores are compacted or propagated into macropores. With the increase of stress level, many micropores are compacted or propagated into macropores, while more newly created micropores are initiated at this time. Therefore, when the
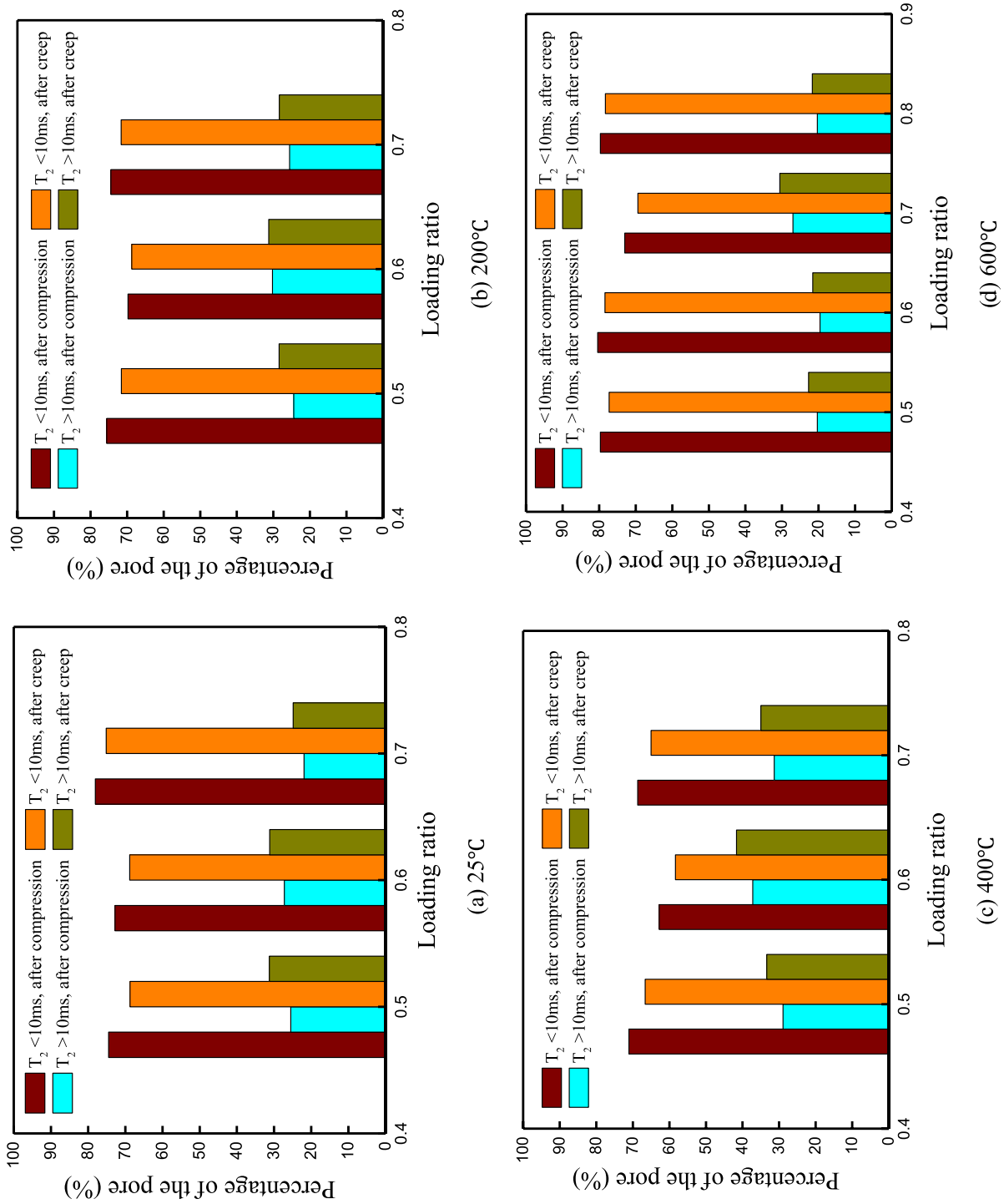
Fig. 14 Percentage of the pore of sandstone samples treated at different temperatures after compression and creep experiments
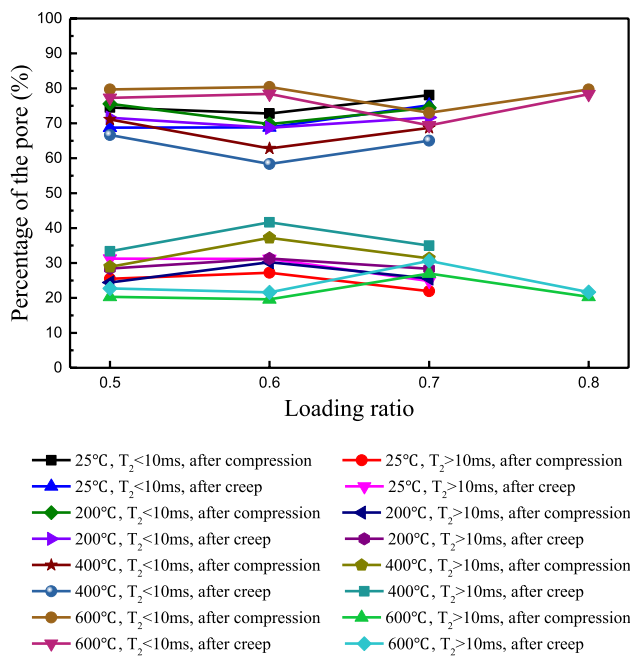
Fig. 15 Relationship between the percentage of the pore distribution and the loading ratio under different conditions

loading ratio is small, as the loading ratio increases, the percentage of micropores decreases, while the percentage of macropores increases. When the temperatures are 25 °C, 200 °C, and 400 °C, as the loading ratio increases from 0.6 to 0.7, the percentage of micropores increases, while the percentage of macropores decreases. When the temperature is 600 °C, as the loading ratio increases from 0.7 to 0.8, the percentage of micropores increases, while the percentage of macropores decreases. This phenomenon indicates that the larger stress levels cause more severe damage to the rock, and more micropores are propagated into macropores in the creep stage. Therefore, when the loading ratio is larger, as the loading ratio increases, the percentage of the micropores increases and the percentage of the macropores decreases.

4 Discussions on the Creep Curves

The creep curve can directly reflect the creep state of the rock sample at different times. Figure 16 shows the creep curves of the multi-stage creep tests of sandstone treated at different temperatures. It can be found from Fig. 16 that under different temperature conditions, the sandstone sample has a transient strain after being loaded, while the attenuation creep strain is not obvious. The stress level has a significant influence on the creep law of sandstone sample at each stage. At the same temperature, as the loading ratio increases, the deformation of the sandstone sample increases significantly. When the loading ratio is 0.5–0.7, the creep

strain is relatively stable and slowly increases over time. During the creep stage at these loading levels, the deformation of sandstone sample is small, leading to a relatively small change in porosity. However, when the loading ratio is 0.8 under the temperature of 25 °C and 200 °C, the sample fails and there is almost no creep strain. As the temperature increases to 400 °C, the creep stage is very short and the creep strain increases rapidly when the loading ratio is 0.8. As the temperature increases to 600 °C, the creep strain is relatively stable and slowly increases over time when the loading ratio is 0.8. This indicates that as the temperature increases, the ductility of the sandstone sample increases.

The deformation of sandstone samples in the creep stage is different under different stress levels or temperature treatment conditions. Figure 17 shows the variation law of creep strain with loading ratio of sandstone samples treated at different temperatures in the creep stage. It can be found from Fig. 17 that the creep strain has an exponential function relationship with the loading ratio. As the loading ratio increases, the creep strain increases, and the incremental rate of the creep strain is greater with an increase in the loading ratio. When the loading ratio increases from 0.5 to 0.6, the creep strain increases relatively slowly. When the loading ratio is greater than 0.6, the creep strain increases faster. Especially, when the temperature is 25 °C, 200 °C, and 400 °C, as the loading ratio increases from 0.6 to 0.7, the creep strain increases faster, increasing by 0.01108%, 0.01464% and 0.01494%, respectively. When the temperature is 600 °C, as the loading ratio increases from 0.7 to 0.8, the creep strain increases from 0.05427 to 0.09183% with an increment of 0.03756%. In addition, under the same loading ratio, as the temperature increases, the creep strain increases significantly. This implies that temperature promotes the deformation of sandstone sample during the creep stage.

Figure 18 shows the variation law of creep strain of sandstone samples in the creep stage with temperature. It can be found from Fig. 18 that the creep strain has a linear function relationship with the temperature. As the temperature increases, the creep strain increases linearly. In addition, the greater the loading ratio, the greater is the increase rate of creep strain. When the loading ratio is 0.5, 0.6 and 0.7, the slopes of the corresponding curves are 1.87, 2.39 and 3.07, respectively. This means that the effect of temperature on the creep strain is more obvious at high stress levels.

The loading ratio and temperature have obvious effects on the creep mechanical properties of sandstone. Comparing Figs. 10 and 17, it can be found that as loading ratio increases, the variation law of the incremental value of porosity is similar to the variation law of creep strain, and both increase exponentially. Similarly, comparing Figs. 11 and 18, it can be found that as temperature increases, the variation law of the incremental value of porosity is similar to the variation law of creep strain, and both increase linearly.
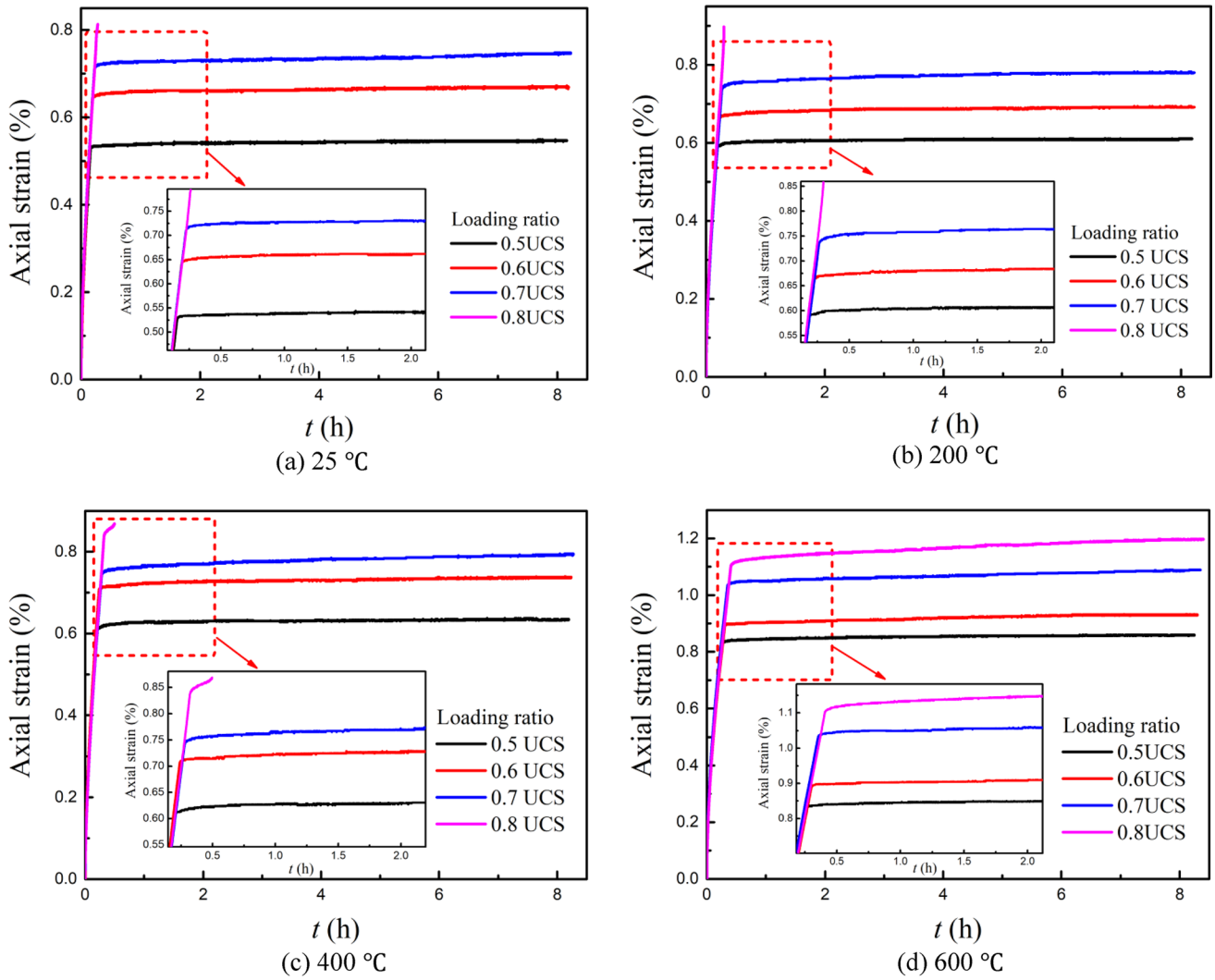
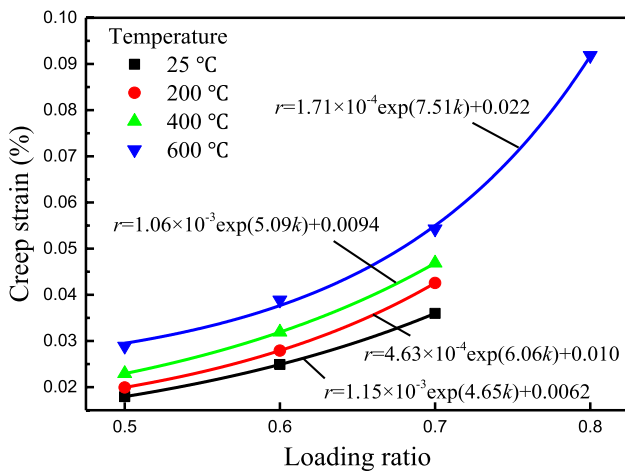**Fig. 16** The curves of the axial strain versus time under different loading ratios

Fig. 17 The variation law of creep strain with loading ratio of sand-stone samples treated at different temperatures
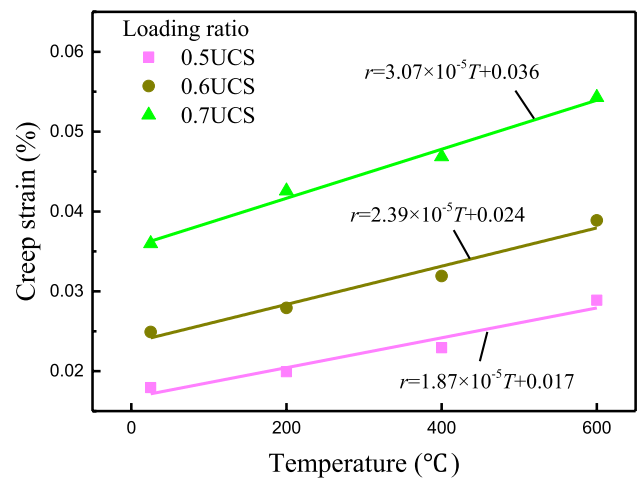

Fig. 18 Relationship between creep strain and temperature under different loading ratios
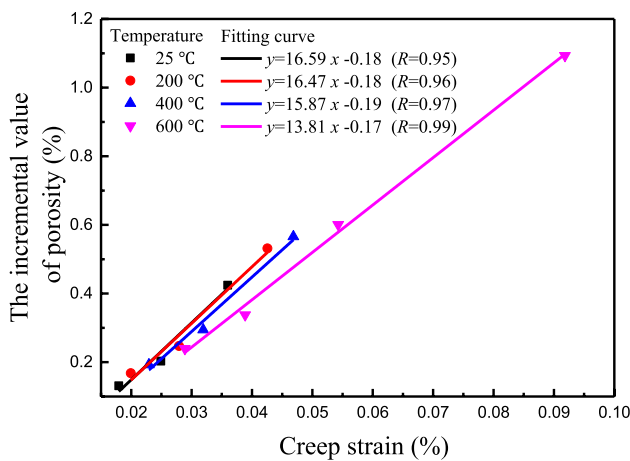
Fig. 19 Relationship between the incremental value of porosity and creep strain under different temperatures

Fig. 20 Relationship between the incremental value of porosity and creep strain under different loading ratios

During the creep stage, the porosity of the sandstone sample changes with the change of the creep deformation. Figure 19 shows the variation law of the incremental value of porosity with creep strain of sandstone samples treated at different temperatures. It is found from Fig. 19 that under the same temperature treatment conditions, the creep strain increases with increasing the loading ratio, leading to a linear increase in the incremental value of porosity. When the loading ratio increases, the sandstone sample enters the yield stage, the creep strain increases; at this time, the creep behavior promotes the initiation of some new microcracks in the sample, leading to the increase of porosity. When the loading ratio increases to a certain level, the sandstone sample is close to failure; at this time, the creep strain increases rapidly, and a large number of microcracks propagate and coalesce to form macrocracks, leading to a rapid increase in the porosity. Heap et al. (2009) and Zhou et al. (2021) also believed that the initiation, propagation and coalescence of microcracks during creep stage are the main reasons for the increase in porosity. They concluded that the increase in stress promotes the initiation of microcracks within the rock, leading to an increase in rock porosity. In addition, it can be found from Fig. 19 that as the temperature increases, the slope of the curve decreases significantly. As the temperature increases from 25 to 600 °C, the slopes of the curves are 16.59, 16.47, 15.87 and 13.81, respectively. It can be concluded that the larger the temperature, the smaller is the effect of creep strain on the incremental value of porosity.

Figure 20 shows the variation law of the incremental value of porosity with creep strain under the different loading ratios. It can be found from Fig. 20 that under the same loading ratio, the creep strain increases with increase in the temperature, leading to a linear increase in the incremental value of porosity. However, as the loading ratio increases, the incremental value of porosity increases faster. As the
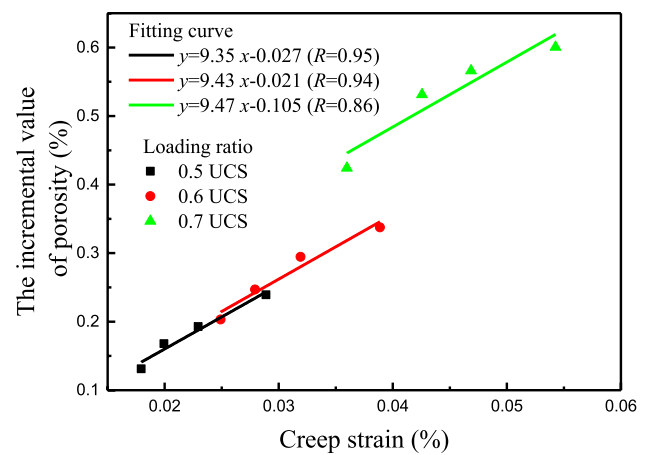
loading ratio increases from 0.5 to 0.7, the slopes of the curves are 9.35, 9.43, and 9.47, respectively. This is because the increase of the loading ratio promotes the more serious damage inside the sandstone sample, which leads to the easier increase of the porosity of the sandstone sample during the creep stage. It is believed that the microscopic deformation and damage characteristics of rock can be indirectly inferred from the change of porosity in the creep stage.

The microstructure characteristics of rocks in high-temperature environment involve many fields such as geotechnical, mining, geology, and energy. The development and utilization of underground space, exploitation of deep mineral resources, and development of geothermal resource areas are all faced with the change of rock mechanical properties in high-temperature environment. Therefore, it is important to study the variation law of porosity during the creep stage of rocks under high-temperature conditions. Based on NMR technology, this paper analyzes the influence of sandstone creep behavior on porosity. It is found that the incremental value of porosity and loading ratio satisfies a good exponential function relationship, while the incremental value of porosity and temperature satisfies a linear function relationship. Through quantitative analysis of NMR parameters, the distribution of porosity of sandstone sample in creep stages under different conditions is discussed. It is found that irrespective of whether after the compression experiment or the creep experiment, the percentage of micropores is relatively large, about 60–80%, while the percentage of macropores is small, about 20–40%. In addition, the creep damage mechanism of sandstone is discussed by combining the change characteristics of the porosity and the characteristics of creep deformation of sandstone sample during the creep stage. It is found that there exists an exponential function relationship between the creep strain and the loading ratio,

while there exists a linear function relationship between the creep strain and the temperature.

Heap et al. (2009) studied the effect of temperature on the creep properties of three sandstones. The experimental temperature varies from 20 to 75 °C. They found that the creep curve at 75 °C is similar to that at room temperature. However, the study in this paper is the creep law of sandstone after high-temperature treatment of 25–600 °C, which is obviously different from the creep law of sandstone under low-temperature conditions. Some differences can be concluded as follows: (1) as temperature increases, the incremental value of porosity increases linearly. It indicates that the temperature promotes the increase of the porosity of sandstone in the creep stage. Moreover, it is found that as loading ratio increases, the incremental rate of porosity also increases. When the loading ratio is 0.5, 0.6 and 0.7, the slopes of the corresponding curves are 1.81, 2.34, and 2.90, respectively. It indicates that the larger the loading ratio, the more sensitive is the incremental value of porosity to temperature. (2) The creep strain has a linear function relationship with the temperature. As the temperature increases, the creep strain increases linearly. In addition, the greater the loading ratio, the greater is the increase rate of creep strain. When the loading ratios are 0.5, 0.6 and 0.7, the slopes of the corresponding curves are 1.87, 2.39 and 3.07, respectively. This means that the effect of temperature on the creep strain is more obvious at high stress levels.

Baud and Meredith (1997) believed that during the creep stage of rock, as stress increases, there are more microcracks in the rock, leading to the increase of porosity. This is similar to the variation law of porosity of sandstone sample obtained in this paper. For example, it can be seen from Fig. 10 that under the same temperature treatment, as the loading ratio increases, the incremental value of porosity of sandstone sample gradually increases, and the incremental rate gradually increases. When the loading ratio exceeds 0.6, severe damage to the sandstone sample is initiated and propagated during the creep stage, and there exists unstable growth of microcracks or microdefects in the sandstone sample. It is believed that when the loading ratio increases, the sandstone sample enters the yield stage and the creep strain increases; at this time, the creep behavior promotes the initiation of some new microcracks in the sample, leading to an increase of porosity. When the loading ratio increases to a certain level, the sandstone sample is close to failure; at this time, the creep strain increases rapidly, and a large number of microcracks propagate and coalesce to form macrocracks, resulting in a rapid increase in the porosity.

Chen et al. (2017) studied the effect of temperature and stress on the creep behavior of granite. They found that the creep strain increases with increasing temperature and deviatoric stress. Yang and Daemen (1997) carried out uniaxial creep experiments of tuff at room temperature and 204 °C, and showed that as temperature increases, the creep deformation of tuff increases. The results of these previous studies are similar to the variation law of creep deformation with stress and temperature in this paper. For example, it can be found from Fig. 17 that the creep strain has an exponential function relationship with the loading ratio. As the loading ratio increases, the creep strain increases, and the increase rate of the creep strain is greater with an increase in the loading ratio. It can be found from Fig. 18 that the creep strain has a linear function relationship with the temperature. As the temperature increases, the creep strain increases linearly. The greater the loading ratio, the greater is the increase rate of creep strain. When the loading ratio is 0.5, 0.6 and 0.7, the slopes of corresponding curves are 1.87, 2.39 and 3.07, respectively. In addition, the paper also analyzes the relationship between the incremental value of porosity and the creep strain. It can be concluded that the larger the temperature, the smaller is the effect of creep strain on the incremental value of porosity. Under the same loading ratio, the creep strain increases with increase in the temperature, leading to a linear increase in the incremental value of porosity. It is believed that the microscopic deformation and damage characteristics of rock can be indirectly inferred from the change of porosity in the creep stage.

5 Conclusions

In this paper, combined with the NMR technology, the measured parameters are used to quantitatively characterize and evaluate the microstructure changes of sandstones treated at different temperatures during the creep stage. The internal damage mechanism and mechanical properties of sandstone treated at different temperatures during the creep stage are discussed, and the following conclusions are finally drawn:

1. In the process of rock creep, due to the propagation of pores, micropores gradually evolve into macropores, leading to a decrease in micropores and an increase in macropores. However, irrespective of whether after the compression experiment or the creep experiment, the percentage of micropores is relatively large, about 60–80%, while the percentage of macropores is small, about 20–40%. When the loading ratio is small, as the loading ratio increases, the percentage of micropores decreases and that of macropores increases. When the loading ratio is large, as the loading ratio increases, the percentage of micropores increases and that of macropores decreases.

2. The incremental value of porosity and loading ratio satisfies a good exponential function relationship, while the incremental value of porosity and temperature satisfies a linear function relationship. The creep strain has an exponential function relationship with the loading ratio, while the creep strain has a linear function relationship with the temperature. Temperature promotes the deformation of sandstone sample during the creep, and the effect of temperature on the creep strain is more obvious at high stress levels.

Declarations

Conflict of interest The authors declare that they have no known competing financial interests or personal relationships that could have appeared to influence the work reported in this paper.

References

Akbulut ZF (2022) Investigation of the change in physical, mechanical, and microstructural properties of Ahlat ignimbrites under the effect of environment and freeze-thawing. Arab J Geosci 15(6):1–11

Alam MM, Hjuler ML, Christensen HF, Fabricius IL (2014) Petrophysical and rock-mechanics effects of CO_2 injection for enhanced oil recovery: experimental study on chalk from South Arne field, North Sea. J Petrol Sci Eng 122:468–487

Baud P, Meredith PG (1997) Damage accumulation during triaxial creep of Darley Dale sandstone from pore volumometry and acoustic emission. Int J Rock Mech Min Sci 34(3–4):24-e1

Chen YL, Ni J, Shao W, Azzam R (2012) Experimental study on the influence of temperature on the mechanical properties of granite under uniaxial compression and fatigue loading. Int J Rock Mech Min Sci 56:62–66

Chen L, Wang CP, Liu JF et al (2017) Effects of temperature and stress on the time-dependent behavior of Beishan granite. Int J Rock Mech Min Sci 93:316–323

Cheng H, Zhou XP, Pan XK, Berto F (2021) Damage analysis of sandstone during the creep stage under the different levels of uniaxial stress using NMR measurements. Fatigue Fract Eng Mater Struct 44:719–732

Daigle H, Hayman NW, Kelly ED, Milliken KL, Jiang H (2017) Fracture capture of organic pores in shales. Geophys Res Lett 44(5):2167–2176

Deng LC, Li XZ, Wang YC et al (2021) Effect of temperature on macroscopic and microscopic properties of sandstone from Qidong coal mine. Rock Mech Rock Eng 55(1):71–90

Dillinger A, Esteban L (2014) Experimental evaluation of reservoir quality in Mesozoic formations of the Perth Basin (Western Australia) by using a laboratory low field nuclear magnetic resonance. Mar Pet Geol 57:455–469

Dwivedi RD, Goel RK, Prasad VVR, Sinha A (2008) Thermomechanical properties of Indian and other granites. Int J Rock Mech Min Sci 45:303–315

Fang WC, Jiang HQ, Li J, Li W, Li JJ, Zhao L, Feng XN (2016) A new experimental methodology to investigate formation damage in clay-bearing reservoirs. J Pet Sci Eng 143:226–234

Gautam PK, Verma AK, Maheshwar S, Singh TN (2018) Thermomechanical analysis of different types of sandstone at elevated temperature. Rock Mech Rock Eng 49(5):1985–1993

Guler S, Turkmenoglu ZF, Varol OO (2021) Thermal shock and freeze-thaw resistance of different types of carbonate rocks. Int J Rock Mech Min Sci 137(2):104545

Heap MJ, Baud P, Meredith PG (2009) Influence of temperature on brittle creep in sandstones. Geophys Res Lett 36(19):1–7

Huang Z, Zeng W, Wu Y et al (2021) Effects of temperature and acid solution on the physical and tensile mechanical properties of red sandstones. Environ Sci Pollut Res 28(3):1–16

Inada Y, Kinoshita N, Ebisawa A, Gomi S (1997) Strength and deformation characteristics of rocks after undergoing thermal hysteresis of high and low temperatures. Int J Rock Mech Min Sci 34(3–4):140

Lei R, Wang Y, Zhang L et al (2019) The evolution of sandstone microstructure and mechanical properties with thermal damage. Energy Sci Eng 7(1):3058–3075

Li M, Liu X (2022) Effect of thermal treatment on the physical and mechanical properties of sandstone: insights from experiments and simulations. Rock Mech Rock Eng 55(6):1–24

Li X, Yin Z (2021) A time-dependent creep constitutive model of deep surrounding rock under temperature-stress coupling. Math Probl Eng 2:1–11

Li N, Wang KW, Zhang G, Wu HL, Zhao LZ, Wu LH, Feng QF, Feng Z (2015) Prediction of gas production in carbonates based on CT analysis and nuclear magnetic resonance (NMR) logging. Pet Explor Dev 42(2):167–174

Li M, Wang D, Shao Z (2020) Experimental study on changes of pore structure and mechanical properties of sandstone after high-temperature treatment using nuclear magnetic resonance. Eng Geol 275(1):105739

Lia H, Zhonga ZL, Liu XR, Sheng Y, Yang DM (2018) Microdamage evolution and macro-mechanical property degradation of limestone due to chemical effects. Int J Rock Mech Min Sci 110:257–265

Liang WG, Xu SG, Zhao YS (2006) Experimental study of temperature effects on physical and mechanical characteristics of salt rock. Rock Mech Rock Eng 39(5):469–482

Liu L, Ji H, Elsworth D, Zhi S, Wang T (2020) Dual-damage constitutive model to define thermal damage in rock. Int J Rock Mech Min Sci 126:104185

Nasseri MHB, Goodfellow SD, Wanne T, Young RP (2013) Thermohydro-mechanical properties of Cobourg limestone. Int J Rock Mech Min Sci 61:212–222

Pan XK, Cheng H, Chen J, Zhou XP (2020) An experimental study of the mechanism of coal and gas outbursts in the tectonic regions. Eng Geol 279:105883

Pan XK, Berto F, Zhou XP (2022a) Creep damage behaviors of red sandstone subjected to uniaxial compression after high-temperature heat treatment using acoustic emission technology. Fatigue Fract Eng Mater Struct 45(1):302–322

Pan XK, Berto F, Zhou XP (2022b) Investigation of creep damage mechanical behaviors of red sandstone considering temperature effect. Fatigue Fract Eng Mater Struct 45(2):411–424

Pathiranagei SV, Gratchev I (2021) Engineering properties of sandstone heated to a range of high temperatures. Bull Eng Geol Environ 80(1):2415–2432

Rios EH, Ramos PFDO, Machado VDF, Stael GC, Azeredo RBDV (2011) Modeling rock permeability from NMR relaxation data by PLS regression. J Appl Geophys 75(4):631–637

Tang Z, Zhai C, Zou Q, Qin L (2016) Changes to coal pores and fracture development by ultrasonic wave excitation using nuclear magnetic resonance. Fuel 186:571–578

Wang X, Huang Q, Lian B et al (2018) Modified Nishihara rheological model considering the effect of thermal-mechanical coupling and its experimental verification. Adv Mater Sci Eng 2018:1–9

Wang X, Huang L, Zhang J (2019) A rheological model of sandstones considering response to thermal treatment. Adv Civ Eng 3:1–9

Xiao F, Jiang D, Wu F et al (2021) Effects of high temperature on the mechanical behaviors of sandstone under true-triaxial unloading conditions. Bull Eng Geol Environ 80:4587–4601

Xiao WJ, Zhang DM, Yang H et al (2022) Evaluation and analysis of sandstone brittleness under the influence of temperature. Geomech Geophys Geo-Energy Geo-Resour 8(1):23–42

Yang CH, Daemen JJK (1997) Temperature effects on creep of tuff and its time-dependent damage analysis. Int J Rock Mech Min Sci 34(3–4):383–384

Yang SQ, Hu B (2018) Creep and long-term permeability of a red sandstone subjected to cyclic loading after thermal treatments. Rock Mech Rock Eng 51:2981–3004

Yao YB, Liu DM (2012) Comparison of low-field NMR and mercury intrusion porosimetry in characterizing pore size distributions of coals. Fuel 95:152–158

Yavuz H (2011) Effect of freeze-thaw and thermal shock weathering on the physical and mechanical properties of an andesite stone. Bull Eng Geol Environ 70(2):187–192

Ye GL, Nishimura T, Zhang F (2015) Experimental study on shear and creep behaviour of green tuff at high temperatures. Int J Rock Mech Min Sci 79:19–28

Yuan SH, Sun Q, Li PF, Geng JS, Zhang H (2022) Fracture properties and dynamic failure of three-point bending of yellow sandstone after subjected to high-temperature condition. Eng Fract Mech 265(15):108366

Zhang H, Sun Q, Geng J et al (2021a) Effect of high temperature on physical properties of yellow sandstone. Heat Mass Transf 57(3):1981–1995

Zhang H, Sun Q, Jia H et al (2021b) Effects of high-temperature thermal treatment on the porosity of red sandstone: an NMR analysis. Acta Geophys 69(7):113–124

Zhang WQ, Wang ZQ, Du Y et al (2022) Effect of high temperature on pore characteristics, yield stress, and deformation property of sandstone. Bull Eng Geol Environ 81:43–54

Zhao Y, Wan Z, Feng Z, Yang D, Zhang Y, Qu F (2012) Triaxial compression system for rock testing under high temperature and high pressure. Int J Rock Mech Min Sci 52:132–138

Zhou XP, Li GQ, Ma HC (2020) Real-time experiment investigations on the coupled thermomechanical and cracking behaviors in granite containing three pre-existing fissures. Eng Fract Mech 224:106797

Zhou XP, Pan XK, Cheng H (2021) The nonlinear creep behaviors of sandstone under the different confining pressures based on NMR technology. Rock Mech Rock Eng 54:4889–4904